Effects of electrode aspect ratio on the reaction rate distribution in microfluidic fuel cell with flow-through porous electrodes

L Li[1,4], Q Xu[2], S Bei[1] and Y She[3]

[1]School of Automotive and Traffic Engineering, Jiangsu University of Technology, Changzhou 213001, China
[2]Department of Computer Science, Changzhou Institute of Technology, Changzhou 213032, China
[3]School of Energy and Environment, City University of Hong Kong, Hong Kong, China

E-mail: liliorigin@jsut.edu.cn

Abstract. In this study, a three-dimensional numerical model has been established and validated for microfluidic fuel cell (MFC) with flow-through porous electrodes. Systematically parametric analyses are performed to evaluate the effects of electrode aspect ratio on the reaction rate distribution in this energy system. Based on the results, the feasibility of improving the utilization degree of the porous electrode by alternating the electrode aspect ratio is demonstrated and optimized electrode aspect ratio is derived for this energy system.

Nomenclature

c^0	inlet concentration, mol m^{-3}
U^0	volumetric flow rate, μL min^{-1}
W	electrode width, mm
L	electrode length, mm
V_{cell}	cell voltage, V
Subscript	
j	species $\{V^{2+},\ V^{3+}, VO^{2+}, VO_2^+$ and $H^+\}$
l	electrolyte
s	electrode

1. Introduction

Increasing power demand in portable electronics is making microfluidic fuel cell (MFC) a promising technology. MFC, also known as membraneless laminar flow-based fuel cell, can operate without a membrane by using the co-laminar nature of the microscale flows for the fuel-oxidant separation purpose [1]. This unique membraneless architecture helps avoid many membrane-related problems,

including complex water management, membrane degradation, high cost and so on [2].

Since the invention of MFC in 2002, a wide array of MFCs has been developed to improve MFC implementations [3-5]. Among them, the flow-through type MFC with porous electrodes reported a class-leading room temperature peak power density [6]. The high power output was mostly owing to the high surface-to-volume ratio of the porous electrodes which enlarged the reaction interfaces greatly. With the rapid increase of the interest in MFC, a number of following works were carried out to boost the cell performance by enlarging the porous electrode volume [7], developing novel porous electrode materials [8] and introducing new cell architectures [9-11].

Porous electrodes are beneficial to the performances of fuel cells. It is optimal to operate porous electrode at the maximum reaction rates everywhere within the porous medium. However, porous electrodes in MFC frequently operate with non-uniform reaction rates. In some parts of the porous electrodes, the reaction rate can be as low as zero [12]. It is thus intriguing to find ways to improve the utilization degree of the porous electrodes. Our previous works show that electrode aspect ratio has a great effect on the reaction rate distribution in the MFC system [13]. Consequently, optimizing electrode aspect ratio is a promising way to improve the utilization degree of the porous electrodes. Work in search of optimized electrode aspect ratio has been performed in the passive direct methanol fuel cells [14]. Yet, detailed analyses have not been conducted to investigate the working mechanisms of the electrode aspect ratio on the reaction rate distribution in microfluidic fuel cell.

In the present work, a 3-D numerical model is developed for MFC with flow-through porous electrodes to evaluate the effects of electrode aspect ratio on the reaction rate distribution and demonstrate the feasibility of improving the utilization degree of the porous electrode by alternating the electrode aspect ratio. Optimized electrode aspect ratio will be derived for this energy system.

2. Numerical model

A 3-D numerical model is established for MFC with flow-through porous electrodes. The computational domains of the fuel cell are shown in figure 1. The anolyte and catholyte contain 2 M V^{2+} in 4 M aqueous H_2SO_4 and 2 M VO_2^+ in 4 M aqueous H_2SO_4, respectively. In the operation, the anolyte and catholyte are pumped into the fuel cell from its two opposite inlets, and then flow through the porous electrodes. The electrodes employed here are made of carbon paper. Electrochemical reactions occur at the electrode-electrolyte interface. After passing the corresponding electrodes, the two streams meet each other in the common middle channel, make a 90°turn and finally flow out of the cell in a laminar format.

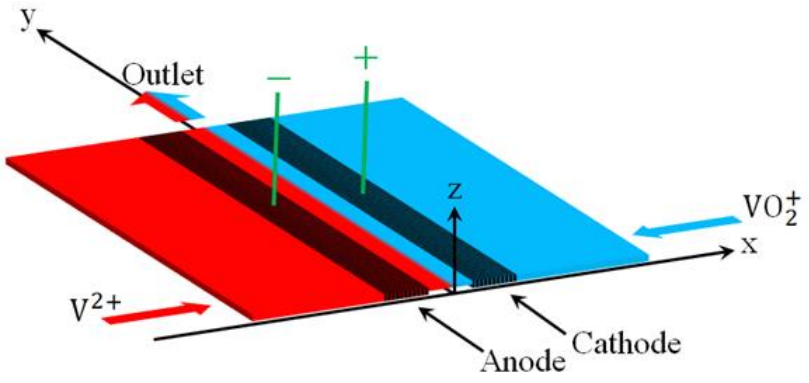

Figure 1. Computational domains of MFC with flow-through porous electrode.

The overall redox reactions considered in this work are:

$$\text{Anode: } V^{2+} \rightarrow V^{3+} + e^- \quad \text{(R1)}$$

$$\text{Cathode: } VO_2{}^+ + 2H^+ + e^- \rightarrow VO^{2+} + H_2O \quad \text{(R2)}$$

In the present model, the following assumptions are adopted:

- The MFC operates under the steady-state conditions;
- The gravity effect and ionic migration are negligible;
- Incompressible fluid flow is assumed;
- Dilute solution approximation is adopted.

2.1. Governing equations

The present 3D numerical model considers the transport of momentum, transport of species, transport of electrons/ions and electrochemical reaction processes. The following governing equations are employed in the numerical model:

2.1.1. Fluid flow. The mass transport is described by:

$$\nabla \cdot \left(\vec{U}\right) = 0 \tag{1}$$

here $\vec{U}$ denotes the velocity vector.

The momentum equation used to describe the fluid flow in the porous electrodes is given below:

$$\nabla P = -\frac{\mu}{K}\vec{U} + \frac{\mu}{\varepsilon}\nabla^2\vec{U} \tag{2}$$

where P is pressure, , K is the permeability, μ is the electrolyte viscosity and ε is the electrode porosity.

The momentum equation used to describe the laminar flow in the middle channel is as follow:

$$\left(\vec{U}\cdot\nabla\vec{U}\right) = -\frac{1}{\rho}\nabla P + \frac{\mu}{\rho}\nabla^2\vec{U} \tag{3}$$

where ρ is the electrolyte density.

2.1.2. Species transport. The species transport in the middle channel is described by:

$$\vec{U}\cdot\nabla c_j - D_j\nabla^2 c_j = 0 \tag{4}$$

where the subscript j indicates the species involved in the electrochemical reactions, including V^{2+}, V^{3+}, VO^{2+}, $VO_2{}^{+}$ and H^{+}. c is the bulk concentration and D is the diffusion coefficient.

The governing equation for the species transport in the porous electrodes is described by:

$$\vec{U}\cdot\nabla c_j - D_j^{eff}\nabla^2 c_j = S_j \tag{5}$$

where D^{eff} refers to the effective diffusion coefficient and S denotes the species source term.

2.1.3. Charge transport. The governing equation for the charge transport in the middle channel can be written as:

$$\nabla\cdot\vec{i_l} = 0, \quad \vec{i_l} = -\sigma_l\nabla\emptyset_l \tag{6}$$

where i_l is the electrolyte current density. σ_l is the electrical conductivity of the electrolyte. $\emptyset_l$ is the electrolyte potential.

The governing equations for the charge transport in the porous electrodes include:

$$\nabla\cdot\vec{i_s} = Q_s, \quad \vec{i_s} = -\sigma_s^{eff}\nabla\emptyset_s \tag{7}$$

$$\nabla\cdot\vec{i_l} = Q_l, \quad \vec{i_l} = -\sigma_l^{eff}\nabla\emptyset_l \tag{8}$$

where i_s is the electrode current density. $\emptyset_s$ is the electrode potential. σ_s^{eff} and σ_l^{eff} are the effective electrical conductivities of the electrode and electrolyte, respectively. Q_s and Q_l are the charge source

terms of the electrode and electrolyte, which can be derived by:

$$Q_s = -Q_l = -ai \tag{9}$$

where i denotes the charge transfer current density, which can be given by the Butler-Volmer equation.

2.2. Numerical procedure

In the simulation, constant flow rate is specified at the inlets for the anode and cathode sides. Constant pressure is set at the outlet of the middle channel. Non-slip condition is given at the channel walls. Reactant concentrations are specified at the inlets for anode and cathode sides. Convective mass transport condition is employed at the outlet of the middle channel. Non-flux condition is assumed at the walls. Electrical potentials of the anode current collector is set to be 0 V and electrical potential of the cathode current collectors is set to be cell voltage. All other boundaries are set to be insulated from electricity. The values of the input parameters are summarized in table 1.

Table 1. Key parameters used in the simulation model.

Parameter	Value	Units
$c^0_{V^{2+}}$	1.89×10^3	$\mathrm{mol\ m^{-3}}$
$c^0_{V^{3+}}$	0.11×10^3	$\mathrm{mol\ m^{-3}}$
$c^0_{VO_2^+}$	1.84×10^3	$\mathrm{mol\ m^{-3}}$
$c^0_{VO^{2+}}$	0.16×10^3	$\mathrm{mol\ m^{-3}}$
$c^0_{H^+}$	8×10^3	$\mathrm{mol\ m^{-3}}$
U^0	60	$\mu\mathrm{L\ min^{-1}}$
V_{cell}	0.7	V

The governing equations of the fluid flow, species transport and charge transport constrained by the boundary conditions are solved by the commercial software COMSOL Multiphysics. Structural meshes are generated. In the electrode subdomains, the mesh size is no larger than 20 $\mu\mathrm{m/cell}$. In the channel subdomains, the mesh size is increased to no larger than 50 $\mu\mathrm{m/cell}$. Relative convergence tolerance is set to be 1×10^{-4}. In the simulation, the equations involved in the fluid flow are first solved and the results are then used to solve the species and charge transports. The final power density is normalized by the anode volume for the comparison convenience among different cases.

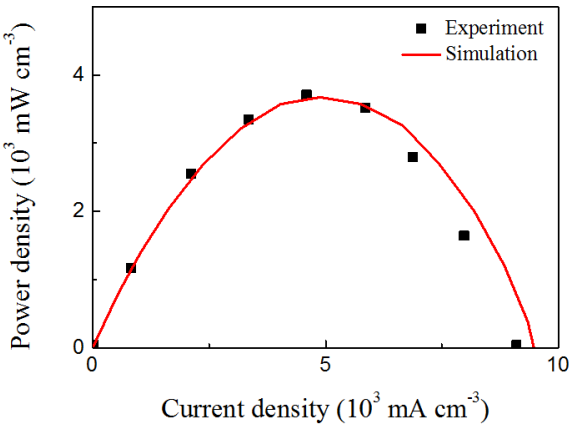

Figure 2. Comparison between the numerically predicted power density curve with the experimental data in [15] (under ambient conditions with a flow rate of 60 $\mu\mathrm{L\ min^{-1}}$).

2.3. Model validation

The developed model is validated by comparing the simulated power density curve with the experimental data in [15]. The operating conditions and geometrical dimensions used in the simulation are the same as those used in the experimental study, where the porous electrode is made of Toray carbon paper (TGPH-090). As shown in figure 2, the simulated and experimental data fit well with each other. In the following analysis, the validated model was employed to investigate the effects of the electrode aspect ratio on the reaction rate distribution in MFC with flow-through porous electrodes.

3. Results and discussion

In the following part, a series of simulation results for the reaction rate distributions in the rectangular electrodes of MFCs are shown first, and then the analysis on the observations of these simulations are given. Here rectangular electrodes are chosen as they are easy to machine and are the most commonly used geometry.

3.1. Characteristics of reaction rate distribution in porous electrode

The reaction rate distributions in the rectangular electrodes with different widths are presented in figure 3. It can be seen that the reaction rate distribution is uniform in the y direction. Yet, in the x direction, the reaction rate decreases rapidly from the electrode/channel interface towards the reactant inlet. In the region close to the reactant inlet, the local reaction rate values are almost zero, which indicates a low utilization degree of the porous electrode material. From figure 3, it can be known that to improve the utilization degree of the porous electrode material, we should decrease the electrode width in the x direction and increase the electrode length in the y direction at the same time, which means to change the electrode aspect ratio.

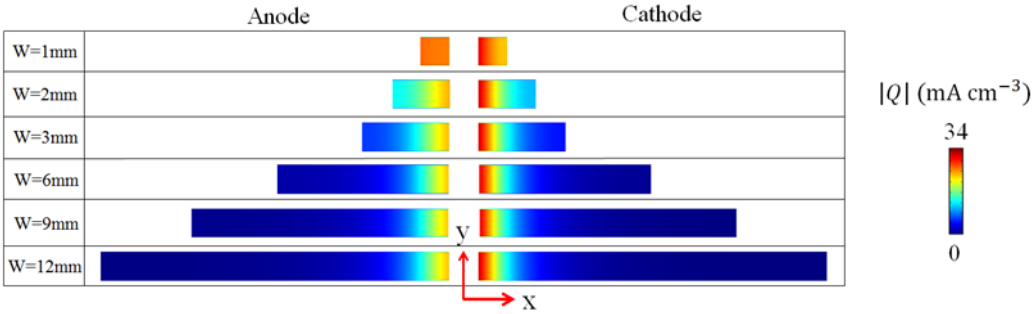

Figure 3. Reaction rate distribution in porous electrodes with different widths.

3.2. Effects of electrode aspect ratio on reaction rate distribution

Decreasing the aspect ratio from W:L=12:1 to W:L=3:4, similar reaction rate profiles can be observed as shown in figure 4. Yet, the non-uniformity degree of the reaction rate distribution decreases, which means an increased utilization degree of the porous electrode. Further decreasing the aspect ratio, a relatively uniform reaction rate distribution was observed in the case with W:L=2:6 and an opposite distribution pattern with reaction rate increasing from the electrode/channel interface towards the reactant inlet was observed in the case with W:L=1:12. The different distribution characteristics of the reaction rate in the electrodes with different aspect ratios can be explained by the different ratios of concentration related activation loss to ohmic loss in these cases.

Corresponding cell performances for these cases are presented in figure 5. We can see that the maximum power output was achieved in the case with W:L=2:6. Compared to the cases with a larger aspect ratio, this case displays a better performance due to the decreased ohmic resistance. Yet, further decreasing the aspect ratio will bring a worse performance as the fluid velocity was too low and thus the increased concentration related activation loss began to dominate the system. From the results, we can obtain an optimal aspect ratio, i.e. W:L=2:6 for the electrode aspect ratio design.

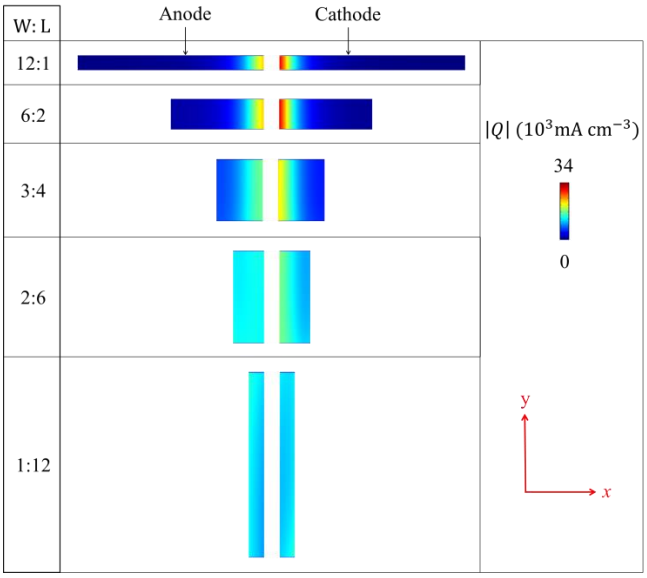

Figure 4. Reaction rate distribution in porous electrodes with different aspect ratios.

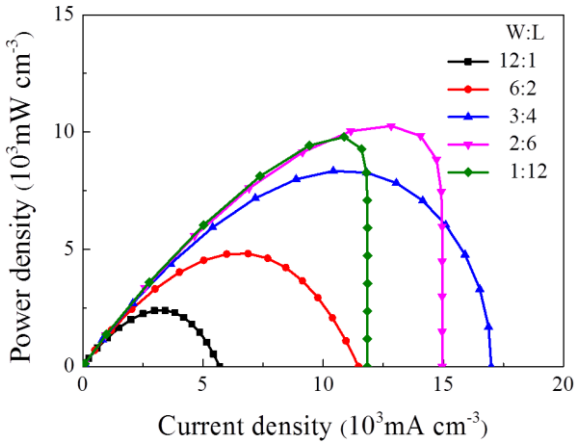

Figure 5. Cell performances of MFCs with different electrode aspect ratios.

4. Conclusions

In this work, effects of electrode aspect ratio on the reaction rate distribution in MFC with flow-through porous electrodes were investigated based on a 3-D numerical model. The results show that it is feasible to improve the utilization degree of the porous electrode by alternating the electrode ratio. Optimized electrode aspect ratio is demonstrated to be W:L=2:6. The present findings about the electrode aspect ratio can be used to optimize the MFC design in the future.

Acknowledgments

This work was financially supported by the Natural Science Foundation of Jiangsu Province (BK20170314), Changzhou Sci & Tech Program (CJ20179016), Jiangsu University of Technology (KYY17008) and Changzhou Institute of Technology 2016 Annual Scientific Research Fund Project (YN1604).

References

[1] Li L, Fan W, Xuan J, Leung M K H, Zheng K and She Y 2017 Optimal design of current

collectors for microfluidic fuel cell with flow-through porous electrodes: Model and experiment *Appl. Energ.* **206** 413-24
[2] Wang Y, Leung D Y C, Zhang H, Xuan J and Wang H 2017 Numerical and experimental comparative study of microfluidic fuel cells with different flow configurations: Co-flow vs. counter-flow cell *Appl. Energ.* **203** 535-48
[3] Nasharudin M N, Kamarudin S K, Hasran U A and Masdar M S 2014 Mass transfer and performance of membrane-less micro fuel cell: A review *Int. J. Hydrogen Energ.* **39** 1039-55
[4] Rashed M K, Mohd Salleh M A, Abdulbari H A, Shah Ismail M H and Izhar S 2015 The effects of electrode and catalyst selection on microfluidic fuel cell performance *Chembioeng Rev.* **2** 356-72
[5] Kjeang E, Djilali N and Sinton D 2009 Microfluidic fuel cells: A review *J. Power Sources* **186** 353-69
[6] Krishnamurthy D, Johansson E O, Lee J W and Kjeang E 2011 Computational modeling of microfluidic fuel cells with flow-through porous electrodes *J. Power Sources* **196** 10019-31
[7] Fuerth D and Bazylak A 2013 Up-scaled microfluidic fuel cells with porous flow-through electrodes *J. Fluids Eng.* **135** 021102
[8] Kwok Y H, Tsang A C H, Wang Y and Leung D Y C 2017 Ultra-fine Pt nanoparticles on graphene aerogel as a porous electrode with high stability for microfluidic methanol fuel cell *J. Power Sources* **349** 75-83
[9] Li L, Nikiforidis G, Leung M K H and Daoud W A 2016 Vanadium microfluidic fuel cell with novel multi-layer flow-through porous electrodes: Model, simulations and experiments *Appl. Energ.* **177** 729-39
[10] Goulet M-A and Kjeang E 2014 Reactant recirculation in electrochemical co-laminar flow-cells *Electrochim. Acta* **140** 217-24
[11] Ibrahim O A, Goulet M A and Kjeang E 2016 In-situ characterization of symmetric dual-pass architecture of microfluidic co-laminar flow cells *Electrochim. Acta* **187** 277-85
[12] Li L, Zheng K, Ni M, Leung M K H and Xuan J 2015 Partial modification of flow-through porous electrodes in microfluidic fuel cell *Energy* **88** 563-71
[13] Li L, Bei S, Xu Q, Zheng K and Zheng Y 2017 Role of electrical resistance and geometry of porous electrodes in the performance of microfluidic fuel cells *Int. J. Energ. Res.* **10** 1-10
[14] Hashemi R, Yousefi S and Faraji M 2015 Experimental studying of the effect of active area on the performance of passive direct methanol fuel cell *Ionics* **21** 2851-62
[15] Kjeang E, Michel R, Harrington D A, Djilali N and Sinton D 2008 A microfluidic fuel cell with flow-through porous electrodes *J. Am. Chem. Soc.* **130** 4000-6